Chinese Chemical Letters 33 (2022) 1817–1830

Contents lists available at ScienceDirect

Chinese Chemical Letters

journal homepage: www.elsevier.com/locate/cclet

Recent development and progress of structural energy devices

Yong Liu[b], Zhongxun Yu[b], Jia Chen[b], Chenxi Li[b], Zhengjie Zhang[a], Xiaoyu Yan[a,*], Xinhua Liu[a,*], Shichun Yang[a,*]

[a] Beihang University, Beijing 100191, China
[b] College of Materials Science and Engineering, Beijing University of Chemical Technology, Beijing 100029, China

ARTICLE INFO

Article history:
Received 13 June 2021
Revised 25 July 2021
Accepted 5 September 2021
Available online 10 September 2021

Keywords:
Structural energy devices
Fuel cells
Lithium-ion batteries
Lithium metal batteries
Supercapacitors

ABSTRACT

In order to fully replace the traditional fossil energy supply system, the efficiency of electrochemical energy conversion and storage of new energy technology needs to be continuously improved to enhance its market competitiveness. The structural design of energy devices can achieve satisfactory energy conversion and storage performance. To achieve lightweight design, improve mechanical support, enhance electrochemical performance, and adapt to the special shape of the device, the structural energy devices develop very quickly. To help researchers analyze the development and get clear on developing trend, this review is prepared. This review summarizes the latest developments in structural energy devices, including special attention to fuel cells, lithium-ion batteries, lithium metal batteries, and supercapacitors. Finally, the existing problems of structural energy devices are discussed, and the current challenges and future opportunities are summarized and prospected. Structural energy devices can undoubtedly overcome the performance bottlenecks of traditional energy devices, break the limitations of existing materials and structures, and provide a guidance for the development of equipment with high performance, light weight and low cost in the future.

1. Introduction

With the rapid development of the global economy and the continuous progress of society, fossil energy sources such as oil and natural gas are gradually depleting. Today environmental pollution and energy crisis are becoming increasingly severe. The development and utilization of new energy is becoming quite urgent [1]. In recent years, the types of new energy devices have become increasingly abundant. The researches on new energy devices such as fuel cells [2–4], lithium-ion batteries [5–7], supercapacitors [8–10] and solar cells [11–14] have developed rapidly in order to transform energy dependence from limited traditional fossil energy to renewable and sustainable resources. The energy conversion and storage of electrochemical devices play an unparalleled important role in new energy technology. In order to be able to fully replace the current traditional fossil energy supply system, the efficiency of electrochemical energy conversion and storage of new energy technologies needs to be continuously improved to enhance their market competitiveness. However, energy conversion and storage usually involve intricate physical interactions and chemical reactions, and related reaction processes usually occur at the interface and inside of the electrode and the electrolyte. The transport behavior and dynamics of electrons, ions, molecules and other carriers are closely related to electrodes, electrolytes and separators. Therefore, the structural design of components such as electrodes, electrolytes, and separators has received high attention from academia and industry, and is the research focus for improving the efficiency of energy conversion and storage of new energy devices. With the rapid development of portable electronic devices and electric vehicles, traditional batteries can no longer meet people's needs. Therefore, more and more attention has been paid to new energy devices that are miniaturized, lightweight, portable and multifunctional. The integrated design of function and structure of energy devices has become one of the current development directions and trends [15–17].

At present, the traditional bulk electrode has encountered a big performance bottleneck. In addition to searching for new electrode materials, the structural design of the electrode can achieve satisfactory energy conversion and storage performance. The reasonable design of the electrode structure can increase the contact area between the electrode and the electrolyte, and improve the overall

* Corresponding authors.
E-mail addresses: yanxiaoyu@buaa.edu.cn (X. Yan), liuxinhua19@buaa.edu.cn (X. Liu), yangshichun@buaa.edu.cn (S. Yang).

https://doi.org/10.1016/j.cclet.2021.09.023
1001-8417/

transmission rate of the battery. From a microscopic point of view, nanostructured electrodes show very powerful advantages. Nanostructured materials have unique properties that are different from their bulk materials. The nanostructured electrode has a high specific surface area, which can expose more active sites and improve electrochemical performance. In addition, the nanostructured electrode can also greatly shorten the transport path of carriers and promote the dynamics of electrochemical reactions. In short, the nanostructure of electrodes is a promising method to achieve high efficiency of energy conversion and storage. From a macro perspective, 3D printing technology can realize the free design of electrode shapes, and can well control the preparation of functional materials with three-dimensional structures. As an emerging advanced manufacturing technology, 3D printing has a great degree of freedom and can quickly create complex structures at a lower cost than traditional methods. So far, several 3D printing technologies have been used to construct electrode structures and improve the electrochemical performance of energy storage devices, such as direct ink writing, stereolithography, inkjet printing, and selective laser sintering. 3D printing technology has the following significant advantages: (1) the ability to prepare complex structures; (2) a high degree of automation, which can realize large-scale production; (3) precise control of micro-sized devices; (4) full printing device can eliminate the negative effects of different preparation processes. 3D printing technology provides tremendous flexibility, which is simply impossible to achieve with traditional manufacturing technology. Without 3D printing, manufacturing parts with arbitrarily complex structures becomes extremely challenging. In short, 3D printing technology represents a promising method for preparing high-performance electrochemical energy storage devices. From the perspective of the entire device, flexible energy storage devices have the advantages of good flexibility, good mechanical stability, small size, light weight, *etc.*, and can also withstand various sizes of deformation. Conventional electronic devices can not meet these requirements effectively due to their volume and rigidity. With the development of wearable electronic devices, people's demand for flexible energy storage devices is increasing. Making energy storage devices into easily portable and curved accessories, or even weaving fibers into clothes, will bring great convenience to life.

In recent years, the technology of functional and structural composite materials has made remarkable progress [18–23]. By improving and innovating the structure of traditional energy devices, new structural energy devices can be obtained. Its primary functions are as follows: (1) Reduce the weight of the device and achieve light weight; (2) From the perspective of mechanics, it can improve mechanical support; (3) The structural design changes the specific surface area, increases the contact area, and improves the electrochemical performance; (4) Considering the adaptability of the shape, it can be adapted to the special shape of the device. Structural energy devices can play a structural role in different applications, and they are becoming more and more popular. Some target applications include unmanned aerial vehicles, new energy vehicles, spacecraft and so on.

Herein, we summarize the latest developments in structural energy devices, including special attention to fuel cells, lithium-ion batteries, lithium metal batteries, and supercapacitors. The structural design of components and the entire device is introduced with emphasis, and various structural designs can achieve satisfactory energy conversion and storage performance. Finally, we discussed the existing problems of structural energy devices, summarized and prospected current challenges and future opportunities. Specifically, structural energy devices can undoubtedly overcome the performance bottlenecks of traditional energy devices, and break the limitations of existing materials and structures. We hope this review will provide great help for those who are interested in structural design of energy devices for further rational design of multifunctional structural energy devices to advance new energy technologies.

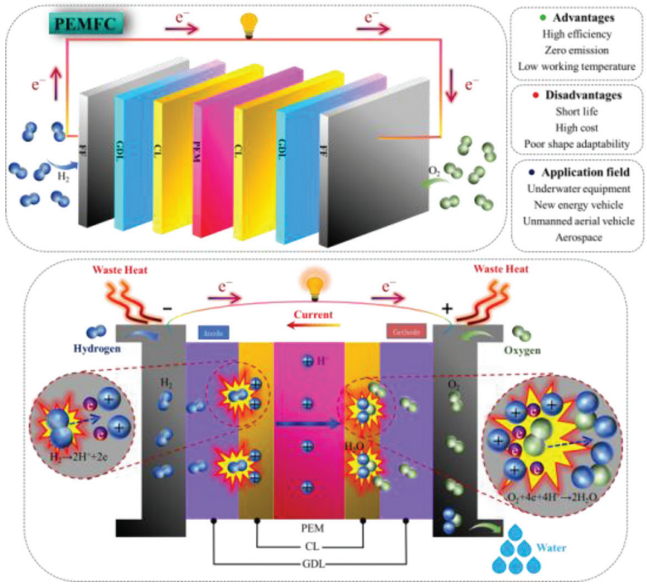

Fig. 1. The basic components and working principle of PEMFC. PEM: proton exchange membrane; CL: catalyst layer; GDL: gas diffusion layer; FF: flow field.

2. Structural fuel cell

A fuel cell is a device that converts the chemical energy stored in the fuel and oxidizer into electrical energy by inputting fuel to carry out an electrochemical reaction. It has the advantages of high energy conversion efficiency, fast startup speed, low noise, and low pollution [24,25]. As a new energy source with great application potential, fuel cells can be used in underwater equipments, new energy vehicles, unmanned aerial vehicles, aerospace and other fields, and have very extensive application prospects. Depending on the type of electrolyte used, fuel cells can be divided into five different types, mainly including proton exchange membrane fuel cells (PEMFC), solid oxide fuel cells (SOFC), phosphate fuel cells (PAFC), alkaline fuel cells (AFC), molten carbonate fuel cells (MCFC) [26–31]. Among them, PEMFC has received the most attention because of its low operating temperature, zero emission, and high efficiency. It has become the fastest growing and most widely used fuel cell [32,33].

2.1. Structural components

PEMFC is mainly composed of membrane electrode assembly (MEA) at the center and flow field plates at both ends, and has a seven-layer structure. MEA is the core component of the cell, which usually consists of three parts: proton exchange membrane (PEM), cathode and anode catalyst layer (CL), and cathode and anode gas diffusion layer (GDL). The fundamental components and working principle of PEMFC are shown in Fig. 1. During the operation of the cell, the wetted hydrogen and oxygen enter the anode flow field and the cathode flow field respectively, diffuse through the GDL, and then reach the CL. Under the action of the anode catalyst, hydrogen loses electrons and undergoes oxidation reaction to generate protons. Among them, protons migrate to the cathode through the PEM, and electrons flow to the cathode through an external circuit to form a current. In the presence of the cathode catalyst, oxygen combines with the protons and electrons reaching the cathode to undergo a reduction reaction to produce water. The

mechanism of the PEMFC reaction can be expressed by the following formula.

$$\text{Anode: } H_2 \rightarrow 2H^+ + 2e^- \quad (1)$$

$$\text{Cathode: } O_2 + 4e^- + 4H^+ \rightarrow 2H_2O \quad (2)$$

$$\text{Cell overall reaction: } 2H_2 + O_2 \rightarrow 2H_2O \quad (3)$$

The PEM is located in the middle of the MEA, which can provide a one-way transmission channel for protons and isolate the anode and cathode. It is a critical component of the fuel cell. Perfluorosulfonic acid membrane is the most widely studied PEM material so far, but its cost is high and its performance at high temperatures deteriorates. Therefore, improving the existing PEM or finding a better one is quite necessary [34–40]. The CL is located on both sides of the membrane, where the electrochemical reaction occurs. Carbon-supported platinum (Pt/C) is considered the best electrocatalyst material. However, Pt is expensive and resource shortage, which greatly increases the cost of PEMFC and restricts its commercial application. Therefore, it is necessary to reduce the amount of metal Pt, thereby reducing the cost of the cell. Improving the catalytic activity of Pt-based catalysts to reduce the amount of Pt, maximizing the utilization of Pt, and finding other cheap metals to replace Pt are the research focuses in recent years. The main research contents include Pt-Metal alloy catalysts [41–44], Pt-based nanostructured catalysts [45–47], Pt-based core-shell structure catalysts [48–51], non-Pt-based catalysts [52,53], *etc.* The GDL can be divided into two layers: the base layer and the microporous layer (MPL). The base layer is generally porous carbon paper or carbon cloth, which is in contact with the flow field plate; while the MPL is usually composed of carbon black and hydrophobic agent polytetrafluoroethylene (PTFE), and is in contact with the CL. The role of the GDL is to support the CL, conduct electrons, uniformly transport the reaction gas to the CL and perform appropriate water management. At present, trying new materials and methods to prepare new MPL is a significant research direction [54–58]. The flow field plate is usually made of metal or graphite, which plays the role of uniformly distributing the reaction gas and timely exhausting water and excess gas. It is the main part of the cell volume and weight. The design and optimization of the flow field structure has been a research hotspot in recent years [59–63], which is of great significance for improving the performance of fuel cells and water and heat management.

PEMFC has attracted the attention of innumerable researchers and achieved certain results. But, further research and exploration are still needed. Nowadays, fuel cells play an important role in new energy vehicles, unmanned aerial vehicles and other fields, but traditional fuel cells are relatively large in weight and volume. One possible way to reduce the weight of cars and unmanned aerial vehicles to achieve light weight is to use structural fuel cells instead of the heavy fuel cell stack [64]. In addition to generating electrical energy, this structural cell can also act as a structural material to withstand mechanical loads and realize the integration of function and structure. Through structural improvement and innovation of traditional fuel cells, structural fuel cells are obtained. The new structural fuel cell can be expected to achieve lightweight design, improve mechanical support, enhance electrochemical performance, and adapt to the special shape of the device. Therefore, it is also necessary to carry out structural design for traditional fuel cells.

The PEM can transfer protons but insulates the electrons. In PEMFC, the PEM not only plays the role of transferring protons, but also acts as a separation between the cathode and the anode. PEM with good performance must meet the following requirements: (1) Strong proton conductivity; (2) High electrochemical and thermal stability; (3) Not easy to deform, and good mechanical properties. The structural design of the PEM is of great significance to improving the overall performance of the fuel cell. The traditional commercial PEM can be replaced by the development of new structural membranes or patterned membranes. Sang *et al.* [65] improved water management by using a prism-patterned Nafion membrane as the polymer electrolyte of MEA. First, the structure of the prism pattern is embossed on the bare Nafion 212 membrane to prepare the prism pattern Nafion membrane. Next, Pt/C catalyst was air-sprayed onto both sides of the prism patterned Nafion membrane to prepare the CL. As a result, it was found that MEA with Nafion membrane with prism pattern showed higher performance compared with traditional MEA. For the MEA of Nafion membrane with prism pattern, performance enhancement is achieved by reducing membrane resistance and increasing electrochemically active surface area. In addition, the asymmetric geometry of the prism structure in the cathode catalyst layer is very easy to remove the water droplets produced. Liu *et al.* [66] prepared a composite PEM containing proton transport channels arranged in a through-plane (TP) direction by solution casting under a magnetic field orientation, as shown in Fig. 2A. Ferrocyanide coordinated poly(4-vinylpyridine) (CP4VP) and phosphotungstic acid (PWA) are used as proton conducting components, and polysulfone (PSf) provides the mechanical strength of the membrane. Under the action of a strong magnetic field, the two water-soluble substances, CP4VP and PWA, combine through electron transfer to form a water-insoluble paramagnetic complex, which is oriented synchronously along the TP direction. Through these aligned and durable short-range proton transport paths, the composite membrane exhibits excellent TP proton conductivity. Compared with other types of hydrocarbon membranes and Nafion® 212 membranes, this composite membrane has excellent proton conductivity, fuel cell performance and durability.

CL is the core component of MEA, that is, the electrochemical reaction site and the transmission channel of gas, water, electrons, protons and other substances. The electrochemical reaction is carried out in the "three-phase zone" composed of catalyst, electrolyte and gas. Therefore, the ideal CL must have enough catalytic active sites to satisfy the "three-phase zone". In addition, there must be sufficiently small mass transfer resistance to facilitate the transfer of electrons, protons and reactants. In order to achieve the above requirements and improve CL performance, the CL structure needs to be improved. Lee *et al.* [67] developed a patterned catalyst layer (PCL) with an in-plane channel structure. The preparation process is as follows: firstly, a patterned poly(urethane acrylate) (PUA) substrate is produced by nanoimprinting technology, and then the surface treatment is performed on the PUA substrate with reverse line pattern. Then, a catalyst slurry is coated on its surface to form a CL with a channel structure in the plane. Finally, it is dried and transferred to the membrane by hot pressing to prepare MEA. The process is shown in Fig. 2B. Studies have shown that the CL with in-plane channel structure can significantly improve the power performance of MEA with low-Pt load due to the enhanced transmission of gas and water. The direct patterning strategy of CL can provide an effective platform for the preparation of CL structures with high structural fidelity, and provide reasonable guidance for the design of high-performance CL. Zeng *et al.* [68] used template-assisted underpotential deposition (UPD) and current displacement methods to deposit ultra-thin Pt skin on PdCo nanotube arrays (NTAs) to construct a 3D-ordered MEA. The advantages of this structure are as follows: (1) ultra-high Pt utilization, because both internal and external surfaces can be used for reactants; (2) enhanced mass transfer due to lower tortuosity; (3) enhanced electronic and ionic conductivity that makes ionomer unnecessary; (4) ultra-high durability due to no carbon carrier. The study found that thanks to the advanced nanostructure, the maxi-

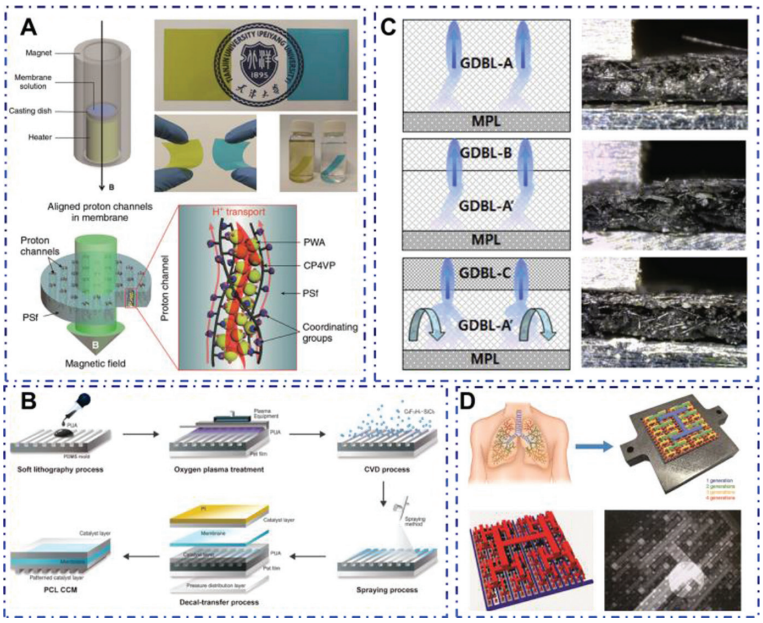

Fig. 2. (A) Diagram of the magnetic-assisted solution casting (top left), photos for NM-45 PC (left in subfigure) and MM-45 PC (right in subfigure) to show appearances (top right), and the conceptual diagrams (bottom). NM-45PC: normal-cast membrane with 45 wt% loading of proton-conducting components; MM-45PC: magnetic-cast membrane with 45 wt% loading of proton-conducting components. Reproduced with permission [66]. Copyright 2019, Nature Publishing Group. (B) Fabrication process of the in-plane channel-structured PCL. Reproduced with permission [67]. Copyright 2018, American Chemical Society. (C) Schematic of the design of the original and modified GDBL structures and cross-sectional digital micrographs of the GDLs. Reproduced with permission [69]. Copyright 2015, Elsevier. (D) The design of lung-inspired flow fields (top), 3D network of the inlet (red) and outlet (blue) branches used in these flow fields (bottom left), and X-ray radiography to inspect the flow fields for structural defects (bottom right). Reproduced with permission [70]. Copyright 2018, Royal Society of Chemistry.

mum power density is 222.5 kW/g, and the Pt load of the cathode is 3.5 μg/cm^2, which is about 14 times higher than the traditional MEA.

GDL has functions such as gas transmission and drainage, heat transfer, current collection, and CL support, especially playing a very important role in water management. It is usually composed of a gas diffusion backing layer (GBDL) with large holes and a MPL with small holes. The ideal GDL needs to have suitable porosity and pore size distribution to ensure the effective diffusion of the reaction gas and the smooth discharge of the product water. Kong *et al.* [69] designed two GDLs with a double-layer GBDL structure, namely GDL-A'B and GDL-A'C (Fig. 2C). GDL-A'B was prepared by stacking GDL-A' and GDBL-B, and GDL-A'C was prepared by stacking GDL-A' and GDBL-C. Both GDL-A and GDL-A' have conventional designs and consist of a single GDBL and a single MPL. The double-layer GBDL structure of GDL-A'B uses the same matrix material, and the porosity of the GDBL-C layer in GDL-A'C is lower than that of the GDBL-A' layer, in order to improve the water retention capacity of GDL-A'C. In order to evaluate the influence of stacking and structural design on self-humidification characteristics, the contact angle, electrical resistance, and vapor permeability of GDL were measured. The electrochemical performance of the fuel cell was also measured under various relative humidity and stoichiometric conditions. It was found that the double-layer structure design of GDBL has a significant impact on the water retention capacity of GDL. Under low humidity conditions, the performance of single cells using GDL-A'C has been significantly improved.

In addition to the structural design of PEM, CL and GDL, the structural improvement or innovation of the flow field plate of the PEMFC can also realize the structuration of the fuel cell. 3D printing technology can be applied in the flow field design of fuel cells to improve the performance of fuel cells. Based on the inspiration of the fractal geometry of the lungs, Trogadas *et al.* [70] used direct metal laser sintering 3D printing technology to design the fractal flow field of the fuel cell to solve the problem of uneven distribution of reaction gas in the cell (Fig. 2D). The newfashioned flow field made by 3D printing is better than the traditional serpentine flow field, and the performance of the cell is better. This is because the reaction gas is more uniformly distributed on the fuel cell catalyst layer. The structural design of structural fuel cells in the future requires 3D printing technology. 3D printing can satisfy the design requirements of lightweight fuel cells while reducing the amount of materials, which is of great significance for reducing the weight of unmanned aerial vehicles or new energy vehicles.

The structural design of fuel cell components can improve the performance of PEMFC, which is of great significance for the future development of low-cost, high-performance, and long-life MEA. In the future, the structural design of fuel cell components can be considered from the following aspects: (1) Optimize the preparation process of PEM, CL, GDL and other components, simplify the preparation process, and increase the possibility of large-scale application of fuel cells. (2) The synergy among PEM, CL, and GDL needs further study. The structural design of the three is coupled to optimize the overall performance of the MEA. (3) The structural design of the fine-sized flow field plate is carried out to improve the performance of the fuel cell. (4) The combination of experiment and simulation is an important research method, and the mathematical model is introduced into the research of structural fuel cells.

2.2. Structural device

A typical structural fuel cell utilizes a skin-core composite sandwich structure, which consists of a thin polymer-based composite skin and a structural fuel cell core, as shown in Fig. 3A. Among them, the structural fuel cell core is composed of metal foam in the outer layer and traditional MEA in the middle layer. The function of the foam core is to provide the shear and compression characteristics required to achieve high sandwich rigidity, and to circulate air and hydrogen at the same time. Sandwich structures are generally used in structural applications because this design mode has high specific bending stiffness and strength [71,72]. The skin-

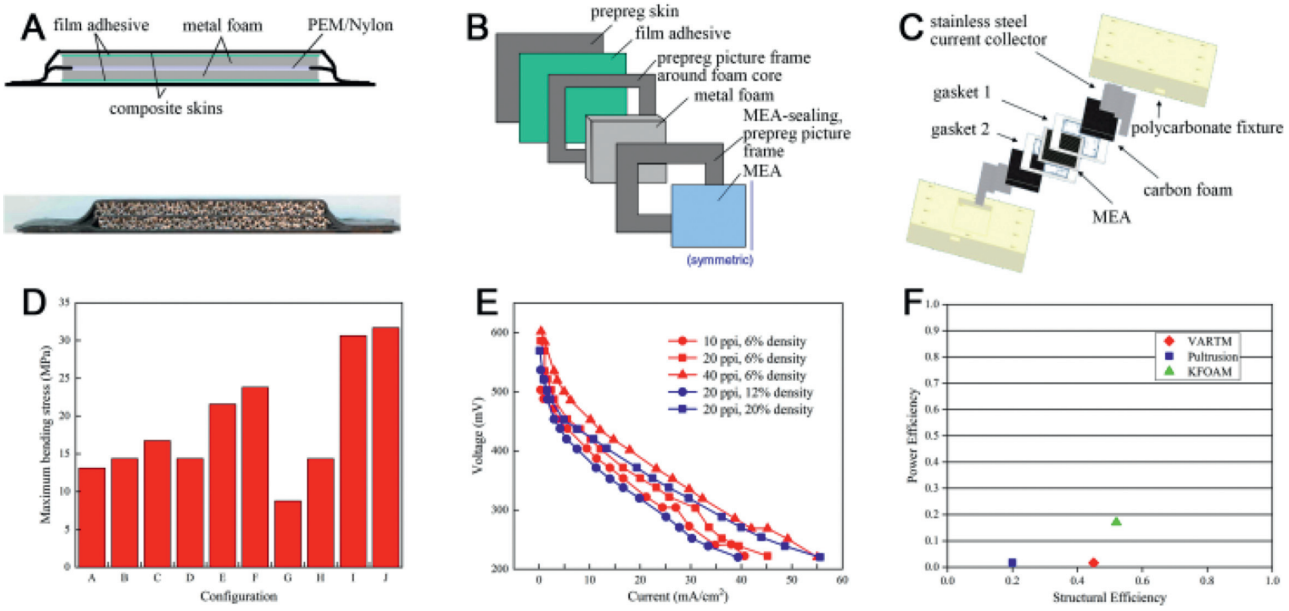

Fig. 3. (A) Cross-section diagram of a multifunctional structural composite fuel cell. (B) Layup used to construct the structural fuel cell. (C) Components of carbon foam fuel cell design. (D) Mechanical performance of various fuel cell samples. (E) Fuel cell performance as a function of foam ppi and density. (F) Multifunctional efficiencies of the fuel cell designs. (A, B, D, E) Reproduced with permission [73]. Copyright 2005, Materials Research Society. (C, F) Reproduced with permission [74]. Copyright 2011, ASME.

core sandwich structural fuel cell is a new type of multifunctional material that can serve as a structural material to withstand mechanical loads while also generating electricity, thereby improving the overall efficiency of the system.

South *et al.* [73] used a skin-core composite sandwich structure to design a functional and structural fuel cell. The components of the structural fuel cell design are shown in Fig. 3B. The thin polymer matrix composite skin on the surface of the fuel cell is made of carbon fiber epoxy resin prepreg. The cell core is composed of two layers of open-pored metal foam aluminum sandwiching a traditional MEA. By changing pores per inch (ppi), density and film adhesive position respectively, different fuel cell samples were designed. The ppi values of samples A, B and C are 10, 20 and 40, respectively. The densities of the samples corresponding to D, E, and F are 6%, 12% and 20%, respectively. The film adhesive positions corresponding to G, H, I and J are No adh., Top-bottom adh., Middle adh., Top-bottom-middle adh., respectively. The mechanical properties of various cell samples were tested through three-point bending experiments. The results found that the maximum bending stress increased with the increase of foam aluminum porosity and foam density, which was caused by the increase of foam material rigidity; the position of the film adhesive between the layers also has a greater impact on the bending strength of the cell, as shown in Fig. 3D. These results demonstrate the importance of designing fuel cell cores with high shear strength. The electrical properties of various cell samples were analyzed through the volt-ampere characteristic curve. It was found that as the porosity and foam density of the aluminum foam increased, the electrical properties of the cell increased, as shown in Fig. 3E. This may be due to the improved interface performance with MEA, thereby reducing ohmic loss; another reason may be that as the permeability of the foam decreases, more electrons flow to the GDL, which will increase the reaction rate of the MEA.

Hilton *et al.* [74] proposed a method that can characterize the design of multifunctional fuel cells to evaluate the potential of structural fuel cells to achieve system level mass savings. The mechanical performance is characterized by the flexural stiffness (M) of the structural fuel cell, the electrical performance is characterized by the power density (P) of the structural fuel cell, and the multifunctional efficiency (σ^{mf}) is characterized by the sum of the structural efficiency (σ^{S}) and power efficiency (σ^{P}) of the structural fuel cell. A solid and lightweight carbon foam (KFOAM) material is used to prepare a structural fuel cell. The components of the fuel cell design are shown in Fig. 3C. On both sides of the membrane electrode assembly, gaskets are used to seal the cell. Then the KFOAM material is placed on both sides of the cell, using stainless steel sheets as the current collector. In addition, vacuum assisted resin transfer molding (VARTM) and pultruded technology (Pultruded) were used to prepare multifunctional fuel cells. The catalyst loading of the membrane electrode assemblies of the three cells is the same. All three cells all adopt a sandwich structure. The relevant data of the three cells in the literature have been sorted out, as shown in Table 1. The research results show that the structural fuel cell based on carbon foam has the best mechanical and electrical properties. This is because the contact pressure of the gas diffusion layer is optimized in the design. The three types of cells have achieved multifunctional efficiencies of 69%, 47% and 22%, respectively. System level mass savings can only be achieved when the value of multifunctional efficiency is greater than 1. Therefore, none of the three fuel cells can achieve system level mass savings, as shown in Fig. 3F. The skin-core sandwich structure belongs to the structuring of the entire fuel cell device, and the structuring of the device can also be achieved by using other more advanced technologies.

Table 1
Performance of three structural fuel cells [74].

Cell design	P (mW/g)	σ^{P}	Mpa mm/g	σ^{S}	σ^{mf}
KFOAM	4.58	0.17	1.30	0.52	0.69
VARTM	0.42	0.016	1.12	0.45	0.47
Pultruded	0.45	0.017	0.50	0.20	0.22

Compared with traditional fuel cells, the sandwich structural fuel cell design uses a very special skin-core composite sandwich structure. Sandwich structural fuel cells can not only generate electricity, but also provide structural support for the system, which has great application potential. Although the electrical performance of sandwich structural fuel cells is not ideal, there is still

a need for research on sandwich structural fuel cells. In the future, the key research of sandwich structural fuel cells will focus on two aspects. One is to optimize the design of the skin-core composite sandwich structure to improve the mechanical and electrical properties of the cell, and the other is to promote the multifunctional design of the structural fuel cell to achieve system level mass savings.

3. Structural lithium battery

3.1. Structural lithium-ion battery

Since its commercialization in 1990, lithium-ion batteries have exhibited the superiorities of high energy density, long-cycle stability, and environmental friendliness. Therefore, it has become one of the most popular power sources for electronic products. Through structural improvement and innovation of lithium-ion batteries, structural lithium-ion batteries can also be obtained. Next, a multiscale concept is proposed to introduce the research progress of structural lithium-ion batteries from nano-micro scale to macro scale.

The structuration of structural lithium-ion batteries is multiscale. The first is the microscopic scale, which includes the structuring of electrode materials. Multi-level structure or coating can be added on the surface of carbon fiber. Carbon fiber is a lightweight and multifunctional composite material, which can not only serve as a battery electrode, but also have a structural strengthening effect. Adding some multi-level structures on the surface of carbon fiber can enhance the specific surface area. From the perspective of improving performance, increasing the specific surface area can bring into full play the electrochemical performance. It is also possible to add coating on the surface of the carbon fiber, and the mechanical strength of the material will change after coating. Structural lithium-ion batteries using commercial carbon fibers as electrodes have relatively low capacity, which limits the further application of structural batteries. The preparation method of coating the surface of carbon fibers with some metal oxides such as Co_3O_4, ZnO, SnO_2, MnO_2 to form composite materials is very economical and simple. These composite materials can be invoked as anode materials for structural lithium-ion batteries. Wang *et al.* [75] used a three-step method to coat the surface of carbon fibers with Co_3O_4 polyhedrons to prepare a new CF@Co_3O_4 composite. The anode material is made of active material CF@Co_3O_4, polyvinylidene fluoride (PVDF) and acetylene black, and copper foil is the electrode current collector. The separator is Celgard 2400 membrane. The electrolyte is a mixture of ethylene carbonate (EC) and diethyl carbonate (DEC) dissolved in $LiPF_6$. The results show that the CF@Co_3O_4 composite material has a porous structure and excellent lithium storage performance. The fabricated battery has a reversible capacity of 420 mAh/g at a current density of 100 mA/g. Han *et al.* [76] coated the surface of carbon fibers with ZnO nanoparticles, and successfully prepared CF@ZnO composite materials as the anode of the structural battery by hydrothermal method. It was found that the structural battery maintained a reversible capacity of 510 mAh/g after 300 cycles at a current density of 100 mA/g. Polyacrylonitrile (PAN) is one of the commonly used carbon fiber precursors. The disordered structure of PAN-based carbon fiber is more suitable for lithium ion insertion. At the same time, the lightweight PAN-based carbon fiber can save volume and mass, and is also considered to be a extremely potential anode material for structural lithium-ion batteries. Therefore, Han *et al.* [77–79] respectively coated the surface of PAN-based carbon fiber with SnO_2, MnO_2 and Co_3O_4, and successfully prepared CF@SnO_2, CF@MnO_2, CF@Co_3O_4 composite materials as the anode of the battery. Li *et al.* [80] prepared a $ZnCo_2O_4$/C coating on carbon fiber, exhibiting enhanced capacity and excellent cycle stability. $ZnCo_2O_4$/C@CF has a unique nanostructure and has potential application value in structural lithium-ion batteries. In addition, nanotube electrodes with hollow structures also belong to the microscopic scale. Liu *et al.* [81] grew $Li_4Ti_5O_{12}$ nanotube arrays on a stainless steel foil substrate based on a template, coated the inner and outer surfaces of $Li_4Ti_5O_{12}$ nanotubes with conductive carbon thin layers, and prepared a self-supporting $Li_4Ti_5O_{12}$-C nanotube array with high conductivity as anode material for lithium-ion batteries. It is found that the prepared $Li_4Ti_5O_{12}$-C nanotube array has excellent rate performance and cycle performance. This is because the diffusion distance of lithium ions is shortened, the hollow structure increases the contact surface, the conductivity is good enough, and the nanotube array has good structural stability.

In addition to the structuration of the anode of the lithium-ion battery, the cathode of the lithium-ion battery can also realize the structuration. Hagberg *et al.* [82] used electrophoretic deposition (EPD) to coat the surface of carbon fibers with $LiFePO_4$, carbon black and PVDF to prepare a structural cathode. It was found that the structural battery has good electrochemical performance, with a specific capacity of about 60∼110 mAh/g. The carbon fiber and the coating have excellent adhesion. This study shows that carbon fibers coated with $LiFePO_4$, carbon black and PVDF can be used as cathode materials for structural batteries, and EPD can be applied to prepare structural cathodes.

On the macro level, 3D printing technology is utilized to prepare lithium-ion battery electrodes. In terms of design dexterity, the advantage of 3D printing is that the shape can be designed freely, which is simply impossible to achieve with traditional manufacturing technology [83]. Researchers Sun *et al.* [84] utilized direct ink writing (DIW) 3D printing technology to prepare interdigital lithium-ion microbatteries composed of high aspect ratio electrode structures. The cathode material of the battery is $LiFePO_4$ (LFP), the anode material is $Li_4Ti_5O_{12}$ (LTO), and the electrolyte material uses $LiClO_4$ with a volume ratio of 1:1 EC and dimethyl carbonate (DMC). The printed 3D interdigital microbattery architectures (3D-IMA) have excellent performance, such as high areal energy density and power density. This is ascribed to the manufacture of a high aspect ratio electrode structure, which has a small footprint while maintaining a relatively small transmission length scale to facilitate the transmission of electrons and ions during charging and discharging. Such microbatteries may find potential applications in micro devices with automatic power supply. Pikul *et al.* [85] reported a lithium-ion microbattery composed of interdigitated three-dimensional bicontinuous nanoporous electrodes with a power density of 7.4 mW cm^{-2} μm^{-1}, which is 2000 times higher than other microbatteries. The microbattery was fabricated by using template-assisted electrodeposition (TAE) 3D printing technology. First, the self-assembled opal template of polystyrene spheres was invoked as the electrode template of the lithium-ion battery. Next, Ni was electrodeposited into the gap of the template, and the template was removed to obtain nickel inverse opal. Finally, a thin layer of Ni-Sn is coated on the nickel support to obtain the battery anode, and lithium manganite $LiMnO_2$ is coated to obtain the battery cathode. The battery microstructure optimizes the transmission of electrons and ions, while reducing the ion diffusion length and resistance in the entire microbattery system, increasing the power density and realizing the microelectronic integration of lithium-ion batteries. Sun *et al.* [86] used a viscous gel-like hybrid ink containing one-dimensional silver nanowires (AgNWs), two-dimensional graphene oxide (GO) nanosheets and LTO nanoparticles to prepare GO-AgNWs-LTO electrodes with a thickness of about 1500 μm through extrusion-based 3D printing technology. The AgNW porous network facilitates the migration of electrons and ions to maintain high conductivity, and the layered porous structure allows complete electrolyte penetra-

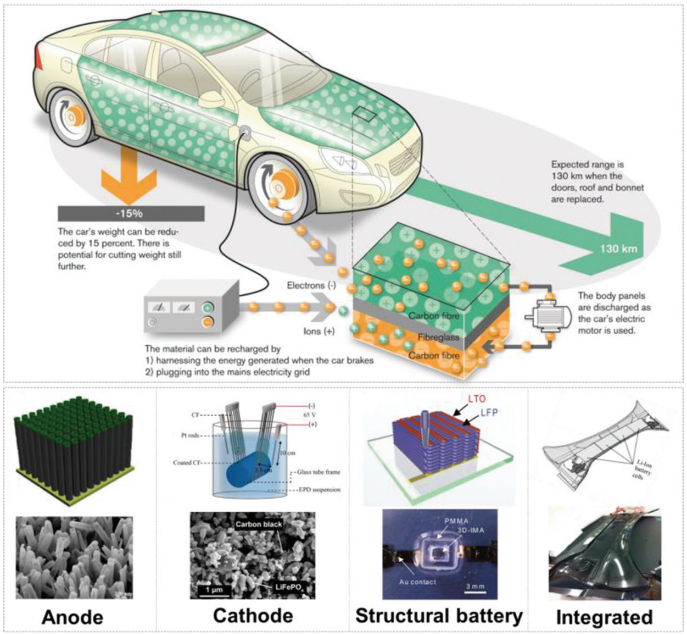

Fig. 4. Multi-scale structural lithium-ion batteries. Reproduced with permission [81]. Copyright 2014, American Chemical Society. Reproduced with permission [82]. Copyright 2018, Elsevier. Reproduced with permission [84]. Copyright 2013, Wiley-VCH.

tion. Interconnected GO scaffolds can provide the required mechanical strength and toughness, which can improve electrode stability. LTO nanoparticles show low volume changes during battery cycling. The results of the study found that the lithium-ion battery with this thick electrode has a specific capacity of 121 mAh/g at 10 C, and an area capacity of 4.74 mAh/cm^2 at a current density of 1.06 mA/cm^2. The capacity retention rate after 100 cycles is approximately 95%. This research work has alleviated the problems of incomplete electrolyte penetration of thick electrodes, poor mechanical properties, and slow electron and ion transfer, providing a valuable reference for the design of thick electrodes for other energy storage devices.

The last is the structuration of the entire device. Similar to structural fuel cells, structural lithium-ion batteries also have a skin-core sandwich structure. Zhang *et al.* [87] prepared a multifunctional lithium-ion battery based on the skin-core sandwich structure and tested it. It was found that the initial capacity of the structural battery was 17.85 Ah, the energy density was 248 Wh/L, and the specific energy was 102 Wh/kg. After 190 cycles of charge and discharge rate of C/3 and 8 cycles of mechanical loading, the capacity retention rate reached 85%. Studies have demonstrated that the concept of a multifunctional structural battery has broad development prospects for the effective use of mass and space in electric vehicles. Carlson *et al.* [88] designed a multifunctional composite automotive component, embedding lithium-ion batteries into the composite component. This multifunctional composite component combines structural functions with electric energy storage, effectively reducing the weight of the system, and successfully demonstrated the potential of using multifunctional components to save space and weight in future electric and hybrid vehicles. Fig. 4 shows multi-scale structural lithium-ion batteries, including the structuration of the anode, the structuration of the cathode, the structuration of the microbattery and the macro body large battery. The structural lithium-ion battery can be applied to the car body in the future to reduce the weight of the car [89].

The complex structural design of the electrodes of lithium-ion batteries brings excellent electrochemical performance, but most of them usually have complex synthesis steps and high costs. The future development of simple, easy and low-cost technology to prepare structural parts is particularly critical. Although 3D printing technology has great flexibility in designing and producing complex architectures, it still faces many challenges. At present, the most developed 3D printing technology can only prepare a single component (electrode or electrolyte), and the one-step printing technology of fully integrated preparation of the entire lithium-ion battery is still very challenging. Designing flexible and variable-shaped lithium-ion batteries to adapt to the shape of the car body is also the focus of future research on structural lithium-ion batteries.

3.2. Structural lithium metal battery

Metal lithium has a high theoretical specific capacity (3860 mAh/g), a low reaction potential (−3.04 V, relative to a standard hydrogen electrode), and light weight, which is considered the holy grail of electrode materials for lithium batteries [90]. Therefore, the research of lithium metal batteries is of great significance to the improvement of energy density. However, metal lithium batteries have serious growth problem of lithium dendrites, which make them face very severe challenges in the process of commercialization. The growth of lithium dendrites is likely to cause the following obstacles, including: (1) The dendrites pierce the separator and contact the positive electrode to cause a short circuit in the battery, raising safety problems. (2) There will be a reaction between lithium metal and the electrolyte, which irreversibly consumes active lithium metal materials and electrolyte, and drastically reduces the coulomb efficiency. (3) During the cycle, the dendritic lithium will fall off the lithium sheet to form a "dead lithium" layer, which will not only reduce the coulombic efficiency, but also increase the internal resistance of the battery and affect the cycle performance. (4) For lithium metal anodes, the volume change during each plating/stripping process is unlimited. Therefore, effectively inhibiting the growth of dendrites and prolonging the cycle life of the battery are the most urgent tasks in the practical application of lithium metal batteries [91].

Since the beginning of the 21st century, methods such as artificial SEI film protection, solid electrolyte, and structural design of metal lithium anodes have provided good solutions to the problem of lithium dendrite growth. Among them, the structural design of lithium metal anode is the focus of research. Through the structural design of the metal lithium anodes, the volume expansion and the current density can be reduced, thereby inhibiting the growth of lithium dendrites and improving the performance of the lithium metal battery. Lin *et al.* [92] designed a layered Li/reduced graphene oxide (rGO) composite material as a lithium metal anode. First, a simple "spark" reaction was developed to generate a uniform nano-gap and partially reduce the GO film, and then Li was uniformly injected into the interlayer space (Fig. 5A). This structure has several obvious advantages. Firstly, the layered structure provides a stable support for lithium stripping/plating, thereby greatly reducing the volume change of the electrode during the cycle. Secondly, rGO has excellent lithium affinity, which can ensure uniform injection and deposition of lithium during the synthesis process and the cycle process, respectively. Thirdly, the top layer of rGO provides an artificial interface that is electrochemically and mechanically stable. Due to these advantages, layered Li/rGO films can improve electrochemical performance. Zhang *et al.* [93] prepared a coral-like silver-coated carbon fiber-based lithium metal anode framework. Using carbon material as the substrate, the silver particles are electroplated on the carbon skeleton by the interval electrophoresis method, and the carbon skeleton with uniformly deposited silver particles is obtained by adjusting the electroplating

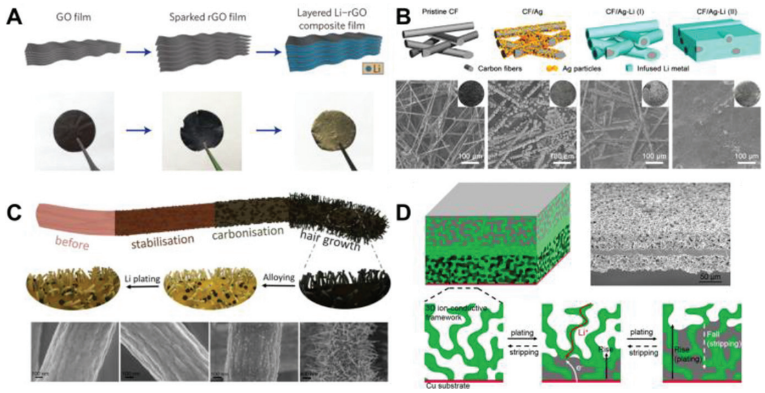

Fig. 5. (A) Fabrication schematic of a layered Li–rGO composite film and corresponding digital camera images. Reproduced with permission [92]. Copyright 2016, Nature Publishing Group. (B) Fabrication schematic diagram of CF/Ag-Li composite electrode and SEM characterization. Reproduced with permission [93]. Copyright 2018, Cell Press. (C) Proposed preparation mechanism for the growth of carbon nanotubes on electrospun fibers and morphology changes during alloying and Li plating. Reproduced with permission [94]. Copyright 2021, Elsevier. (D) Schematic for the process of Li plating and stripping in the 3D garnet-type ion-conductive framework. Reproduced with permission [96]. Copyright 2018, National Academy of Sciences.

current density and the time interval. Due to the affinity of silver and lithium, perfect contact between molten lithium metal and the carbon framework can be achieved, as shown in Fig. 5B. The results of the study found that the battery can be cycled stably for 400 cycles without degradation at a current density of 1 mA/cm^2, and it exhibits good cycle performance compared with a symmetrical battery of bare lithium.

The 3D structure of the lithium metal anode support has a stable electron transfer framework and a porous structure that can achieve higher capacity, which can reduce volume changes and improve the overall performance during Li plating/stripping. Therefore, Liu *et al.* [94] demonstrated the design of a 3D structural lithium metal anode by electrospinning. The anode is continuous carbon nanofibers with cobalt-modified nitrogen-doped carbon nanotubes grown *in situ*, as shown in Fig. 5C. The porous and independent structure can enhance the resistance to the stress caused by the inherent volume change during the lithium plating/stripping process, thereby significantly increasing the charge/discharge rate and stabilizing the cycle performance. The binary Co-Li alloy phase is formed during the initial discharge process, which creates more active sites for the nucleation and uniform deposition of Li. Related characterization and density functional theory simulation calculations show that the conductive and uniformly distributed cobalt-decorated carbon nanotubes have a layered structure, which can effectively reduce the local current density and absorb Li atoms more easily, thereby achieving more uniform Li nucleation during the plating process. Xue *et al.* [95] proposed a 3D porous core-shell fiber scaffold as a lithium metal anode, which is composed of well-dispersed SiO_2, TiO_2 and carbon. It was found that even at an ultra-high current density of 10 mA/cm^2, amorphous SiO_2 and TiO_2 can still control the nucleation and deposition of metallic lithium inside the porous core-shell fiber. In addition, the hollow fibers and interconnected conductive skeletons can achieve rapid electron and ion transport during cycling, high Li loading, and structural integrity of the matrix. After being paired with $LiNi_{0.5}Co_{0.2}Mn_{0.3}O_2$ (NCM) cathode, the full battery exhibits high discharge capacity and excellent cycle performance. The stable cycle performance of up to 200 cycles can be obtained at 10 C. Yang *et al.* [96] used a garnet-type ion-conducting framework as the matrix of the lithium metal anode, studied its plating/stripping behavior, and proved that it is a safe and dendritic-free solid lithium metal anode (Fig. 5D). The study found that the solid lithium metal anode in the main body of garnet has excellent cycle stability, which can be cycled for more than 300 h under the condition of 0.5 mA/cm^2, and the overpotential is small.

A good SEI film requires high lithium ion conductivity, high elastic modulus, and a thin and compact film structure. The concentration of the electrolyte, the composition of the electrolyte, additives, *etc.* will have a great impact on the properties of the SEI film and the deposition behavior of lithium, so the modification of the electrolyte is very important. At present, researchers are committed to finding suitable electrolyte additives to modify the SEI film of lithium metal anodes. It is desirable to construct a highly stable SEI layer to suppress the formation of lithium dendrites and extend the life of the battery. Li *et al.* [97] designed a gradient SEI structure with C–F bonds rich surface and LiF rich bottom layer by using a novel bisfluoroacetamide (BFA) as multifunctional electrolyte additive. Due to the polar C–F bond on the SEI surface, Li^+ is easily adsorbed. Due to the low Li^+ diffusion barrier of LiF, Li^+ can be quickly transported to the lithium anode through the LiF rich layer. This novel gradient SEI structure achieves fast Li^+ kinetics and uniform Li deposition. In addition, BFA molecules can adjust the Li^+ solvation structure by reducing the free solvent in the electrolyte, improve the stability of the electrolyte, and prevent the extensive degradation of the electrolyte on the cathode surface, thereby forming a uniform and stable cathode electrolyte interphase (CEI). The results of the study found that BFA additives can achieve dendrite-free lithium plating/stripping in symmetric batteries, with lower overpotential and higher cycle stability. The full cells containing BFA additives showed excellent rate performance and capacity retention after 200 cycles. This work provides a very effective strategy for exploring effective electrolyte additives to inhibit lithium dendrites and protect the cathode structure. It also provides a certain reference for the SEI design of other metal batteries. Wang *et al.* [98] reported that crown ether was used as an electrolyte additive and verified that the complexation between lithium ions and crown ether made lithium metal batteries exhibit long cycle life. When the crown ether is introduced into the electrolyte, the lithium ion/crown ether complex can reduce the surface concentration of lithium ions and form a larger primary crystal nucleus. During the plating process, the complex not only reduces the accumulation of lithium ions on the surface of the dendrite, but also isolates the carbonate electrolyte to form a uniform and dense SEI film, which inhibits the growth of lithium dendrites and improves the cycle performance of the battery. Qi *et al.* [99] proposed a multifunctional electrolyte additive (potassium perfluorinated sulfonate) to inhibit the growth of lithium dendrites. Firstly, K^+ can form an electrostatic shielding on the surface of the lithium anode to inhibit the further growth of lithium dendrites. Then, potassium perfluorinated sulfonate acts as a con-

ductive salt to increase the activity of the electrolyte and reduce the potential for lithium nucleation. Thirdly, the perfluorosulfonate anion can not only change the Li^+ solvation sheath structure to reduce the desolvation energy barrier and increase the ion mobility, but also can be partially decomposed to form an excellent SEI. The addition of perfluorosulfonate also helps to form a thin and uniform CEI layer. These synergistic effects effectively inhibit the formation of lithium dendrites, thereby prolonging the cycle performance.

Compared with the traditional bulk electrode, the structural lithium metal anode can not only significantly reduce the volume change of the electrode during the cycle, but also adjust the behavior of lithium ion plating/stripping to inhibit the growth of lithium dendrites. The structural matrix is very important for the lithium metal anode, which helps to realize a dendritic-free and highly conductive lithium metal anode. It is of vital importance to further optimize the structural matrix and develop a simpler and low-cost method to prepare structural composite lithium metal anodes.

4. Structural supercapacitor

4.1. Structural electrode and electrolyte

Due to its high power density, long cycle life, and short supply time, supercapacitors have made breakthroughs in advanced energy applications. The charge storage in supercapacitors utilizes the electrostatic field formed at the electrode/electrolyte interface. Through reasonable structural design of electrodes or electrolytes, the energy conversion and storage performance of supercapacitors can be improved. Structural supercapacitors are a new type of supercapacitors, which have attracted the attention of a growing number of scientific researchers. Structural supercapacitors are usually composed of two functional structural electrodes and polymer electrolyte [100].

The structuration of structural supercapacitors is also multiscale. The first is the microscopic scale, such as multi-level structure design on the surface of nanomaterials. Carbon fiber has the advantages of large specific surface area, good electrical conductivity, light weight, high specific strength and specific modulus, and good corrosion resistance. Therefore, it is a very ideal electrode material and plays a very important role in the development of structural supercapacitors. Carbon nanotubes (CNT) have excellent mechanical, electrochemical and thermal properties. CNT can be grown on the surface of carbon nanofibers (CNF) prepared by electrospinning [101], which is an effective method to improve the performance of structural supercapacitors. Li *et al.* [102] used CNF with CNT growing on the surface as the electrode material and polyethylene glycol diglycidylether (PEGDGE) as the solid resin electrolyte to prepare a new structural supercapacitor. It was found that CNF/CNT electrodes have better capacitance performance than ordinary CNF electrodes, with a capacitance of about 3.35 mF/cm^2. The estimated Young's modulus of the CNF/CNT sample is 271 GPa, while the estimated value of the CNF sample is 145 GPa. The growth of CNT not only enhances the capacitance of the structural supercapacitor, but also improves its mechanical properties. This study shows that CNF has great potential as an electrode material for structural supercapacitors. Javaid *et al.* [103] used VARTM for the first time to prepare a structural supercapacitor. The carbon fiber loaded with graphene nanosheets is used as the electrode material, and the filter paper is used as the separator material. The polymer electrolyte is made of the diglycidylether of bisphenol A epoxy (DGEBA) and triethylenetetramine (TETA) crosslinker, and $LiClO_4$ and propylene carbonate (PC) are added to enhance ion mobility. Graphene nanosheets have a large specific surface area, and loading them on the carbon fiber mats can improve the charge storage capacity on the electrode and increase the energy density and power density. The results demonstrate that when the content of graphene nanosheets is 10 wt%, the power density of the fabricated supercapacitor is 47 W/L, the energy density is 0.26 Wh/L, and the in-plane shear modulus is 3.1 GPa. It is a novel and easy-to-implement method to use carbon fibers loaded with graphene nanosheets as electrodes for structural supercapacitors. This method can enhance the versatility of structural supercapacitors, and provide new ideas for further research on structural supercapacitors. Qian *et al.* [104] injected carbon aerogel (CAG) into carbon fiber fabric to form a cohesive but porous overall structure for the development of multifunctional electrodes. CAG modification can increase the surface area of the carbon fiber fabrics, thereby improving electrochemical performance. Continuous CAG can be applied as the nano-reinforced material of the matrix to form a layered structure that can enhance mechanical properties. The study also found that the in-plane shear strength and modulus were increased by 4.5 times, which improved the mechanical properties. CAG modified structural carbon fiber fabric has excellent potential in multifunctional energy storage applications.

Next, the improved design of the electrolyte material of the supercapacitor can realize the structuration. For example, adding mesoporous particles to the electrolyte improves the performance of structural supercapacitors. Javaid *et al.* [105] fabricated a structural supercapacitor by a resin infusion under the flexible tooling (RIFT) method. Activated carbon fiber is used as the electrode, glass fiber is used as the separator, and cross-linked PEGDGE is used as the electrolyte. Mesoporous SiO_2 particles are added to the electrolyte as a reinforcing agent. When mesoporous SiO_2 particles are added to the polymer electrolyte, the SiO_2 particles tend to form aggregates, thereby providing excellent ion transport performance. The results showed that fiber activation and the addition of mesoporous SiO_2 particles improved the performance of the structural supercapacitor, and its energy density and shear modulus were increased. The prepared supercapacitor has a power density of 34 W/kg, an energy density of 0.12 Wh/kg, and a shear modulus of 1.75 GPa. Wang *et al.* [106] utilized PVDF, lithium trifluoromethanesulfonate (LiTf) and epoxy resin as raw materials to prepare a new solid adhesive polymer electrolyte. A structural supercapacitor was prepared by the vacuum bagging method, using carbon-based electrodes and an epoxy-based adhesive polymer electrolyte. The research results indicate that the fabricated structural supercapacitor has acceptable mechanical strength and excellent electrochemical performance. The maximum specific energy can reach 2.64 Wh/kg, and the tensile strength can reach 80 MPa. In addition, the response of electrochemical properties to tensile stress was further studied. It is found that the specific power and specific energy increased slightly with the increase of tensile stress before the sample fractured. Shirshova *et al.* [107] prepared a bicontinuous multifunctional electrolyte by mixing a commercial epoxy resin with an ionic liquid based Li-containing electrolyte. The study found that under the condition of 30 wt% structural resin and 70 wt% ionic liquid based electrolyte, the prepared structural electrolyte had a room temperature ionic conductivity of 0.8 mS/cm and a Young's modulus of 0.18 GPa. The performance improvement can be ascribed to the formation of a bicontinuous structure of the structural electrolyte. The two-phase system spontaneously forms a bicontinuous nanostructure. One phase provides ionic conductivity, and the other phase improves structural rigidity.

From a macro perspective, 3D printing technology can also be applied to prepare supercapacitor electrodes. In recent years, 3D printing has become a method of manufacturing unique electrodes with high aspect ratios and arbitrary shapes. Liu *et al.* [108] used direct metal laser sintering (DMLS) 3D printing technology to obtain porous stainless steel scaffolds, and then combined MnO_2, Mn_2O_3, poly(3,4-ethylenedioxythiophene) (PEDOT) and polystyrene sulfonic acid (PSS) to obtain MnO_x-PEDOT:PSS film layer on the

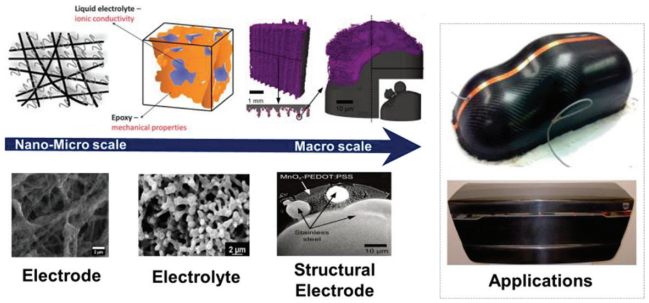

Fig. 6. Multi-scale structural supercapacitors from nano-micro to macro scale. Reproduced with permission [100]. Copyright 2014, Royal Society of Chemistry. Reproduced with permission [102]. Copyright 2018, Springer. Reproduced with permission [107]. Copyright 2013, Royal Society of Chemistry. Reproduced with permission [108]. Copyright 2016, Wiley-VCH.

surface of the 3D printed stainless steel scaffolds by the co-electrodeposition method. MnO_x-PEDOT:PSS films are utilized as composite electrodes for structural pseudocapacitors. In the case of porous scaffolds, since the accessible surface area increases, the active material forms a relatively thin layer. By combining the porous stainless steel scaffold with a thinner membrane layer, this can improve the surface area and enhance the conductivity of electrons to increase the efficiency of the charge and discharge process. The new method combining 3D printing and co-electrodeposition has realized structural pseudocapacitors with higher surface capacitance, longer cycle performance and lower resistance, and a new perspective on the development of 3D printed pseudocapacitors with structural load-bearing capacity has been proposed. It is also of great significance to the development of other 3D printing energy storage devices. Li *et al.* [109] used DIW printing technology to prepare 3D graphene electrodes. First, graphene ink was printed layer by layer to form a 3D structure. After freeze drying and chemical reduction treatment, a 3D graphene electrode with a specific shape was obtained. The gel electrolyte was prepared by dissolving polyvinyl alcohol (PVA) powder in deionized water and then adding H_2SO_4. The unique 3D graphene structure enables the new miniature supercapacitors to have excellent performance, such as high specific capacitance, long cycle life, stable mechanical flexibility and integration with microelectronic devices.

Fig. 6 shows multi-scale structural supercapacitors from nano-micro to macro scale. Structural supercapacitors have great possibilities in electric vehicles, aerospace and portable electronic products. As an application example, the LEDs of a full size trunk lid for a Volvo S80 are powered by structural supercapacitors.

Reasonable structural design of electrodes and electrolytes to develop structural supercapacitors with higher power density, energy density and elastic modulus is still a hot research direction in the future. Similar to lithium-ion batteries, the most advanced 3D printing technology can only prepare a single component (electrode or electrolyte) of a supercapacitor, and the one-step printing technology for fully integrated preparation of the entire supercapacitor is still very challenging.

4.2. Flexible and stretchable supercapacitor

Traditional supercapacitors are usually made of rigid plates and appear bulky, which is disadvantageous for many applications. For example, portable, highly integrated devices, they have to be small, light and highly flexible [110–112]. Therefore, flexible equipment has become a development trend today [113–115].

Flexible supercapacitors can be designed into a variety of shapes, and the shapes of their devices are diversified, such as fiber line, ring, sheet. Fibrous supercapacitors have received more and more attention from researchers, due to their light weight, small size, high flexibility, and strong weavability [116,117]. Cai *et al.* [118] utilized electrodeposition to synthesize composite fibers of highly oriented multi-walled carbon nanotubes (MWCNT) and polyaniline (PANI), and covered a layer of gel electrolyte on the MWCNT-PANI composite fibers. Two composite fibers were twisted to prepare a linear supercapacitor, as shown in Fig. 7A. The study found that the specific capacitance of the prepared linear supercapacitor was as high as 263 mF/cm. Lightweight, high strength, high flexibility and weavability provide it with promising applications in various fields. Chen *et al.* [119] used carbon nanotube fibers and sheets to prepare an electric double-layer capacitor fiber with a coaxial structure (Fig. 7B). They serve as the two electrodes of the capacitor, and a polymer gel is added between them to act as an electrolyte. The unique coaxial structure can reduce the contact resistance between the two electrodes, and quickly transport ions between the two electrodes, which are beneficial to achieve higher electrochemical performance. The experimental results found that the maximum discharge capacitance can reach 59 F/g, and it has been maintained in good condition under high current. This energy storage fiber material is also flexible and stretchable, can be commonly applied in electronic textiles, and has very huge application potential. Qu *et al.* [120] developed hollow fiber electrodes including reduced graphene oxide/conductive polymer composite fibers with PVA/H_3PO_4 gel as the electrolyte, and prepared a new type of fibrous supercapacitor (Fig. 7C). The formation of the hollow structure is due to the release of gas during the reduction reaction of graphene oxide. The hollow structure inside the fiber will increase the specific surface area, thereby increasing the contact interface between the electrode and the electrolyte and promoting the transfer of charges. It is found that this new type of fiber supercapacitor has a specific capacitance as high as 304.5 mF/cm^2, an energy density as high as 6.8 $\mu Wh/cm^2$, and long-life stability. Fiber supercapacitors can be woven into soft textiles, which are particularly promising for portable and wearable electronic devices. Liao *et al.* [121] incorporated fluorescent dye particles into aligned MWCNT sheets through a cospinning process, and performed a rolling process to convert the sheets into fibers. Then, two fluorescent fiber electrodes were coated with a layer of aqueous gel electrolyte. Finally, two fiber electrodes were twisted together to prepare a new type of multicolor fluorescent supercapacitor fiber (Fig. 7D). The fluorescent component in the dye introduces a fluorescent indicator function to the supercapacitor fiber, which shows great hope for flexible and wearable devices used in dark environments. In addition, the color fluorescent supercapacitor fiber can also maintain very good electrochemical performance during the cycle of bending and charge-discharge processes. In addition to fibrous linear supercapacitors, supercapacitors can also be made into rings and sheets to satisfy new wearable applications and other emergency requirements. Wang *et al.* [122] wound the aligned CNT/PEDOT:PSS composite sheets onto an elastic polymer ring to prepare a ring-shaped supercapacitor. The study found that the prepared toroidal supercapacitor showed a high specific capacitance of 134.8 F/g, and could maintain excellent electrochemical performance under the action of expansion and pressure. Due to its high flexibility and elasticity, the same ring-shaped supercapacitor can meet substrates of various sizes and irregular shapes (Fig. 7E). Sun *et al.* [123] prepared thin and flexible supercapacitors through advanced slicing technology. Sheet supercapacitors have uniform surface and compact interface, and have excellent electrochemical performance. Simultaneously, their thickness is adjustable. The study found that the specific capacitance of the sheet supercapacitor is as high as 248 F/g, and it can maintain good electrochemical performance before and after bending. As an application demonstration, the researchers fixed three series-connected thin supercapacitors on the fingernails to light up commercial LED light (Fig. 7F), which showed its huge application potential. The

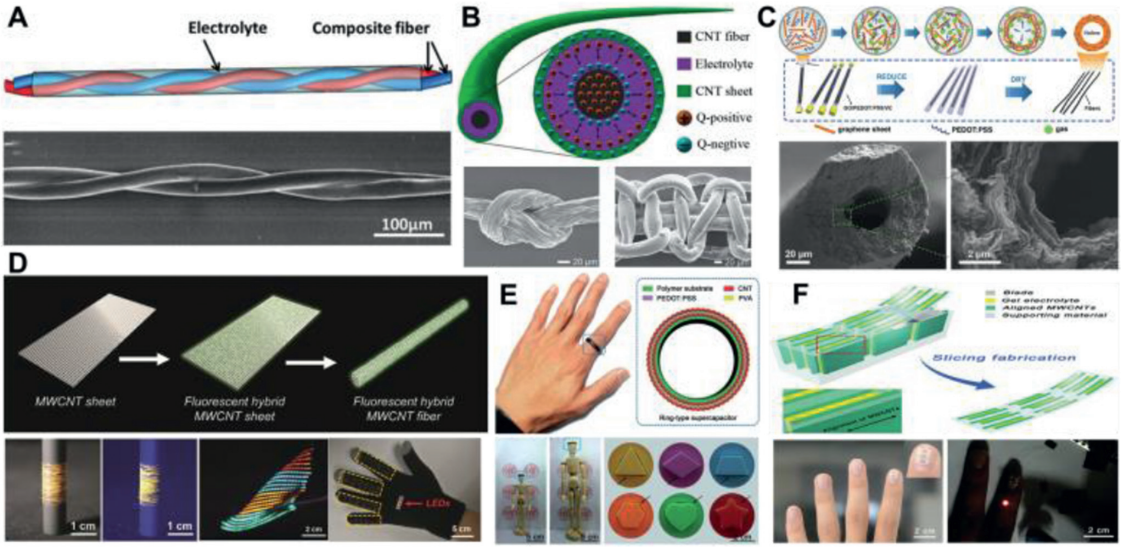

Fig. 7. (A) Schematic illustration and SEM image of two aligned MWCNT–PANI composite fibers twisted into a fiber supercapacitor. Reproduced with permission [118]. Copyright 2013, Royal Society of Chemistry. (B) Schematic illustration of a fiber supercapacitor with coaxial structure (top), SEM image of a fiber being made into a knot (bottom left) and SEM image of several fibers being woven into a textile structure (bottom right). Reproduced with permission [119]. Copyright 2013, Wiley-VCH. (C) Schematic illustration of preparation of a fiber supercapacitor with hollow structure (top), and cross-sectional SEM images of the hollow composite fibers at low and high magnifications, respectively (bottom). Reproduced with permission [120]. Copyright 2016, Wiley-VCH. (D) Schematic diagram of the preparation process of the fluorescent fiber electrode (top), photographs of continuously prepared fluorescent fiber under natural light and ultraviolet, photograph of fluorescent supercapacitor fibers with four colors woven into a black textile under ultraviolet, and fluorescent supercapacitor fibers woven into a glove to power red light-emitting diodes. Reproduced with permission [121]. Copyright 2018, Wiley-VCH. (E) Photograph and schematic illustration of the structure of the ring-shaped supercapacitor (top), and photographs showing that the ring-shaped supercapacitor can be worn on the substrates of various sizes and irregular shapes (bottom). Reproduced with permission [122]. Copyright 2016, Royal Society of Chemistry. (F) Schematic diagram of manufacturing the thin supercapacitor through slicing method (top), and photographs of the thin supercapacitors powering red-light-emitting diode in the dark (bottom). Reproduced with permission [123]. Copyright 2016, Wiley-VCH.

slicing method has the advantages of low cost, small individual difference and controllable thickness, and can be extended to other thin energy storage devices with high performance.

Supercapacitor fibers can be woven into textiles with high performance, which have great potential in the application of wearable electronic devices. Sun *et al.* [124] developed a large-area supercapacitor textile with high energy storage performance by designing a novel layered conductive structure. Hong *et al.* [125] utilized a multichannel spinneret with two internal parallel nozzles for electrode inks and a larger external nozzle for carrying gel electrolyte to continuously produce supercapacitor fibers of several kilometers length and high productivity through a one-step process. PEDOT:PSS and CNT are mixed to prepare high-viscosity electrode ink for two fiber electrodes. The mixture of chitosan and PVA is used as gel electrolyte, because chitosan is easy to solidify and PVA has higher mechanical strength. The supercapacitor fibers produced also show high flexibility, structural stability and electrochemical stability, and are further woven into a soft scarf by knitting machine (Fig. 8A), which is expected to realize wearable applications. Carbon nanotube arrays with unique gradual structure can be used as electrode materials for supercapacitors. Zhao *et al.* [126] developed a new type of compressible carbon nanotube array (CCNA) material by imitating the gradient structure of the mouth of the giant squid. This CCNA material has a unique highly crosslinked gradual structure in the vertical direction, can withstand different degrees of compressive strain, and has high reversible compressibility and excellent conductivity. By using CCNA as the electrode, a new type of compression sensing supercapacitor was prepared, which can store energy and sense changes in external strain. As an application demonstration, multiple compression sensing supercapacitors are integrated into the circuit to make a multifunctional device. When different amounts of pressure are applied on the flexible integrated watchband, the LEDs of different colors are lightened (Fig. 8B). Nanowire arrays can also be used as electrode materials for supercapacitors. Ning *et al.* [127] synthesized $NiCoO_2$/NiCoP nanowire arrays directly grown on nickel foam, and embedded NiCoP nanoparticles into amorphous $NiCoO_2$ on a single nanowire. The unique and novel structural design combines the characteristics and advantages of metal phosphides and metal oxides. Firstly, the design of the self-supporting $NiCoO_2$/NiCoP material on the foamed nickel improves the conductivity of the electrode and reduces the internal resistance. Secondly, the morphology of the nanowire array shortens the ion transmission path and increases the specific surface area. Thirdly, the combination of highly active NiCoP and stable $NiCoO_2$ significantly improves the specific capacitance and cycle performance. With $NiCoO_2$/NiCoP nanowire array/Ni as the positive electrode and activated carbon as the negative electrode, the assembled all-solid-state supercapacitor exhibits excellent flexibility. At the same time, two devices connected in series can light up 21 red LED indicators. With the increasing demand for portable and wearable electronic devices, flexible and transparent supercapacitors have also become a new generation of energy storage devices [128]. Based on the fractal network structure of leaf veins, Chen *et al.* [129] prepared Au/polypyrrole (PPy) transparent flexible electrodes through chemical etching, UV lithography, sputtering deposition of Au metal film, stripping of photoresist, and electrochemical deposition of PPy (Fig. 8C). Then, researchers used PVA/LiCl gel as the electrolyte and wrapped the electrolyte with a frame made of acrylic double-sided adhesive to assemble a transparent supercapacitor. The assembled transparent supercapacitor has a visible light transmittance of 45% at a current of 1 mA and a surface capacitance of 5.6 mF/cm^2. In addition, the transparent supercapacitor also has excellent electrochemical stability and mechanical flexibility, and is expected to be widely applied in transparent wearable electronic products.

Although the preparation of flexible supercapacitors has made rapid progress and made huge research results, there are still many

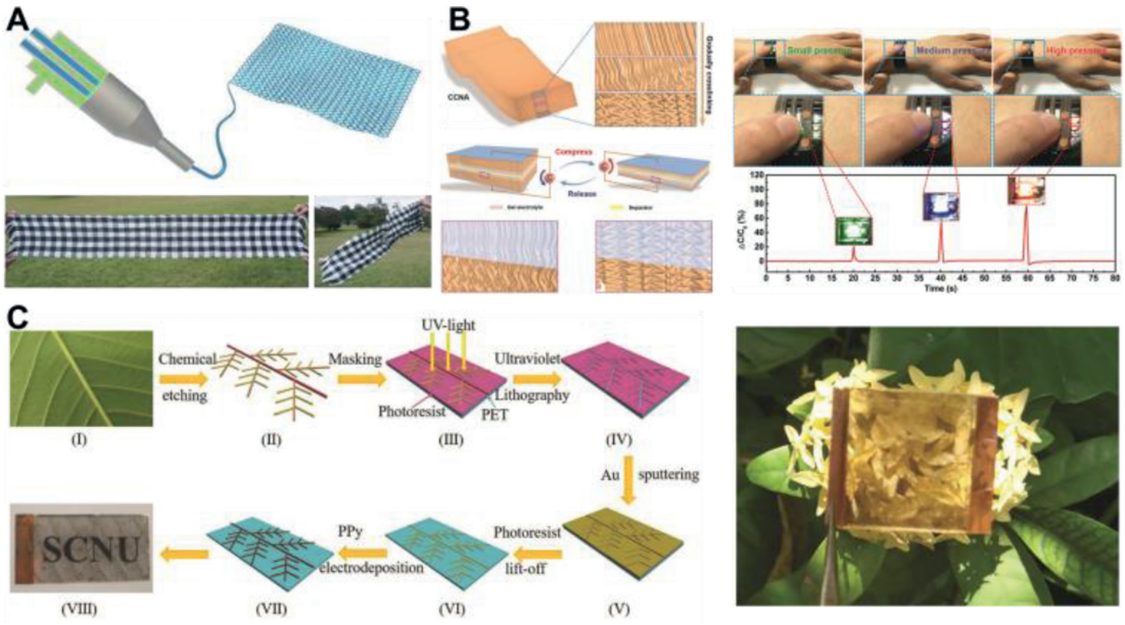

Fig. 8. (A) Schematic of the continuous fabrication of supercapacitor fibers toward energy storage textiles (top), a supercapacitor scarf by weaving the supercapacitor fibers with cotton yarns (bottom left), and the supercapacitor scarf demonstrated to be flexible (bottom right). Reproduced with permission [125]. Copyright 2019, Springer. (B) Schematic diagram of the CCNA with gradually crosslinking structure, Schematic diagram of the compression sensing supercapacitor function as a strain sensor before and after compressing, and different pressures being applied on the flexible integrated circuit to light up different colored LEDs. Reproduced with permission [126]. Copyright 2020, Wiley-VCH. (C) Schematic diagram of the fabrication process of PPy/Au network electrode, and photograph of supercapacitor demonstrating high transparency. Reproduced with permission [129]. Copyright 2019, Wiley-VCH.

unsolved problems to be explored. The electrochemical performance of flexible supercapacitors is far from meeting the needs of practical applications. For flexible fiber supercapacitors, while maintaining their inherent high specific power density unchanged, it is still important to enhance their capacitance and energy density. Still need to further explore and develop other new materials for mass production of flexible electrodes. At present, flexible supercapacitor fibers can only be woven on a limited area with small machines or by hand. Using commercial machines to weave fiber supercapacitors over a large area is a huge challenge. Flexible design of device shapes to develop the diversification of supercapacitor shapes is still a significant research direction.

5. Summary and outlook

Traditional energy devices have encountered performance bottlenecks. In addition to finding new and suitable materials, the structural design of energy devices can achieve satisfactory energy conversion and storage performance. By improving and innovating the structure of traditional energy devices, new structural energy devices can be obtained. Structural energy devices are expected to achieve lightweight design, improve mechanical support, enhance electrochemical performance, and adapt to the special shape of the device. This review puts forward the concept of structural energy devices and summarizes the latest developments in structural energy devices, including fuel cells, lithium-ion batteries, lithium metal batteries, and supercapacitors. First, the structural fuel cell is introduced, focusing on the structural components and the skin-core sandwich structure of the entire device. Next, the research progress of structural lithium-ion batteries and structural lithium metal batteries in recent years is also summarized. The key developments of structural lithium-ion batteries are summarized from a multiscale perspective, and structural design of lithium anode for lithium metal batteries is highlighted. The latest developments in structural electrodes and structural electrolytes of supercapacitors are also summarized in the view of multiscale. Finally, flexible supercapacitors with diversified shapes are shown. Each structural energy device has its own merits and drawbacks, as shown in Fig. 9.

Structural energy devices can effectively save system weight and volume, and improve performance. Therefore, they have broad development prospects in the fields of unmanned aerial vehicles, new energy vehicles, and aerospace. For example, structural batteries are expected to be used in the body of unmanned aerial vehicles or new energy vehicles to reduce the weight of unmanned aerial vehicles or cars and improve their overall performance. Structural energy devices have attracted the attention of a growing number of researchers and made certain progress, but they still face enormous challenges. The structuration of batteries and supercapacitors in the future depends on structural design and material selection. The design of the structure requires novel and unique technologies. For example, 3D printing technology can topologically optimize the complex structural designs. It can satisfy the needs of lightweight design while reducing the amount of materials, thereby achieving structural weight reduction. 3D printing technology is increasingly favored by people, and will continue to be applied in the structural design of structural batteries and supercapacitors in the future. At present, the most developed 3D printing technology can only prepare a single component (electrode or electrolyte) of a battery or capacitor, and the one-step printing technology of fully integrated preparation of the entire device is still challenging. Besides, 4D and 5D printing technologies are also hopeful to be used in the structural design of energy devices. In order to rationally design the structure of the component or the entire device, an advanced, low-cost, and environmentally-friendly synthesis strategy is urgently needed. The choice of materials is also an important issue. The structuration of batteries and supercapacitors in the future will require materials with low density, low cost and better performance. It is still essential to search for new materials with further improved electrochemical properties. In order to expand structural devices from the laboratory to the industrial scale, there is an urgent need to develop low-cost

Structural energy devices			
Structural fuel cell	Structural lithium-ion battery	Structural lithium metal battery	Structural supercapacitor
High efficiency	High energy density	High energy density	High power density
Zero emission	High working voltage	High specific capacity	Large capacity
Low working temperature	High charging efficiency	Low reaction potential	Short charge/discharge time
Short life	Small self-discharge	Light weight	Long cycle life
High cost	Long cycle life	Poor safety performance	Low energy density
Poor shape adaptability	High cost	Poor chemical stability	High cost

Fig. 9. Various structural energy devices.

and mass-produced technical strategies. In addition, structural devices must be further stacked and packaged to meet the urgent needs of high energy density, high power density, and high safety. In addition to structural fuel cells, structural lithium-ion batteries, structural lithium metal batteries and structural supercapacitors, structural energy devices can also be extended to structural air batteries, structural flow batteries, structural solar cells, *etc.* This has far-reaching significance for the development of structural energy devices in the future. With the efforts and struggles of generations of scientific researchers, a variety of structural energy devices will bring earth-shaking changes to the world, and promote better progress and development in the fields of new energy vehicles, aerospace, and electronic equipment. In short, structural energy devices have very huge development opportunities, and the exploitation of new integrated batteries and supercapacitors with high performance, light weight, and low cost is still a key research direction in the future.

Declaration of competing interest

The authors declare that they have no known competing financial interests or personal relationships that could have appeared to influence the work reported in this paper.

Acknowledgments

This work was supported in part by the National key R&D Program of China (No. 2018YFB0105200), and National Natural Science Foundation of China (No. U1864213). The authors also wish to acknowledge Xin Li and Jihao Wang for detail revisions.

References

[1] S. Chu, A. Majumdar, Nature 488 (2012) 294–303.
[2] C.Y. Lee, A.C. Taylor, S. Beirne, G.G. Wallace, Adv. Mater. Technol. 4 (2019) 1900433.
[3] M.K. Debe, Nature 486 (2012) 43–51.
[4] D. Banham, S. Ye, K. Pei, et al., J. Power Sources 285 (2015) 334–348.
[5] X. Yu, Y. Liu, H. Pham, et al., Adv. Mater. Technol. 4 (2019) 1900645.
[6] S. Gao, X. Zhan, Y.T. Cheng, J. Power Sources 410 (2019) 45–52.
[7] T.F. Yi, Y.R. Zhu, W. Tao, et al., J. Power Sources 399 (2018) 26–41.
[8] T. Ni, S. Wang, J. Shi, et al., Adv. Mater. Technol. 5 (2020) 2000268.
[9] A. Eftekhari, L. Li, Y. Yang, J. Power Sources 347 (2017) 86–107.
[10] H. Liang, J. Lin, H. Jia, et al., J. Power Sources 378 (2018) 248–254.
[11] M. Rawat, E. Jayaraman, S. Balasubramanian, S.S.K. Iyer, Adv. Mater. Technol. 4 (2019) 1900184.
[12] S. Razza, F. Di Giacomo, F. Matteocci, et al., J. Power Sources 277 (2015) 286–291.
[13] X. Fan, Y. Rui, X. Han, et al., J. Power Sources 448 (2020) 227405.
[14] S. Ahmad, X. Guo, Chin. Chem. Lett. 29 (2018) 657–663.
[15] B.K. Deka, A. Hazarika, J. Kim, Y.-.B. Park, H.W. Park, Int. J. Energy Res. 41 (2017) 1397–1411.
[16] P. Ladpli, R. Nardari, F. Kopsaftopoulos, F.-.K. Chang, J. Power Sources 414 (2019) 517–529.
[17] K. Moyer, N.A. Boucherbil, M. Zohair, J. Eaves-Rathert, C.L. Pint, Sustain. Energy Fuels 4 (2020) 2661–2668.
[18] L. Christodoulou, J.D. Venables, Jom-J. Miner. Metals Mater. Soc. 55 (2003) 39–45.
[19] L.E. Asp, E.S. Greenhalgh, Compos. Sci. Technol. 101 (2014) 41–61.
[20] S. Leijonmarck, T. Carlson, G. Lindbergh, et al., Compos. Sci. Technol. 89 (2013) 149–157.
[21] E.S. Greenhalgh, J. Ankersen, L.E. Asp, et al., J. Compos Mater. 49 (2014) 1823–1834.
[22] A. Javaid, K.K.C. Ho, A. Bismarck, et al., J. Compos Mater. 50 (2015) 2155–2163.
[23] S. Yin, Z. Hong, Z. Hu, et al., J. Power Sources 476 (2020) 228532.
[24] V. Mehta, J.S. Cooper, J. Power Sources 114 (2003) 32–53.
[25] O.Z. Sharaf, M.F. Orhan, Renew. Sustain. Energy Rev. 32 (2014) 810–853.
[26] E. Antolini, E.R. Gonzalez, J. Power Sources 195 (2010) 3431–3450.
[27] R. Ebrahim, M. Yeleuov, A. Ignatiev, Adv. Mater. Technol. 2 (2017) 1700098.
[28] D. Frattini, G. Accardo, A. Moreno, et al., J. Power Sources 352 (2017) 90–98.
[29] B. Shri Prakash, R. Pavitra, S. Senthil Kumar, S.T. Aruna, J. Power Sources 381 (2018) 136–155.
[30] K. Strickland, R. Pavlicek, E. Miner, et al., ACS Catal. 8 (2018) 3833–3843.
[31] R. Wu, Y. Song, X. Huang, et al., J. Power Sources 401 (2018) 287–295.
[32] X.X. Wang, M.T. Swihart, G. Wu, Nat. Catal. 2 (2019) 578–589.
[33] Y. Wang, D.F. Ruiz Diaz, K.S. Chen, Z. Wang, X.C. Adroher, Mater. Today 32 (2020) 178–203.
[34] K. Charradi, Z. Ahmed, P. Aranda, R. Chtourou, Appl. Clay Sci. 174 (2019) 77–85.
[35] S. Jahangiri, İ. Aravi, L. Işıkel Şanlı, Y.Z. Menceloğlu, E. Özden-Yenigün, Polym. Adv. Technol. 29 (2018) 594–602.
[36] S.-.W. Kim, S.Y. Choi, H.-.W. Rhee, J. Membr. Sci. 566 (2018) 69–76.
[37] C. Klose, M. Breitwieser, S. Vierrath, et al., J. Power Sources 361 (2017) 237–242.
[38] F. Ng, D.J. Jones, J. Rozière, et al., J. Membr. Sci. 362 (2010) 184–191.
[39] P. Salarizadeh, M. Javanbakht, S. Pourmahdian, RSC Adv. 7 (2017) 8303–8313.
[40] F. Xu, S. Mu, M. Pan, J. Membr. Sci. 377 (2011) 134–140.
[41] P.A. Henry, L. Guétaz, N. Pélissier, P.A. Jacques, S. Escribano, J. Power Sources 275 (2015) 312–321.
[42] E.B. Tetteh, H.Y. Lee, C.-.H. Shin, et al., ACS Energy Lett. 5 (2020) 1601–1609.
[43] X. Xiong, W. Chen, W. Wang, J. Li, S. Chen, Int. J. Hydrogen Energy 42 (2017) 25234–25243.
[44] Y. Zhou, D. Zhang, J. Power Sources 278 (2015) 396–403.
[45] M. Dou, M. Hou, Z. Li, et al., J. Energy Chem. 24 (2015) 39–44.
[46] W.S. Jung, B.N. Popov, Catal. Today 295 (2017) 65–74.
[47] Z. Yan, B. Li, D. Yang, J. Ma, Chin. J. Catal. 34 (2013) 1471–1481.
[48] U. Aslam, S. Linic, ACS Appl. Mater. Interfaces 9 (2017) 43127–43132.
[49] S.T. Hunt, M. Milina, A.C. Alba-Rubio, et al., Science 352 (2016) 974–978.
[50] X. Tian, J. Luo, H. Nan, et al., J. Am. Chem. Soc. 138 (2016) 1575–1583.
[51] K.C. Wang, H.C. Huang, C.H. Wang, Int. J. Hydrogen Energy 42 (2017) 11771–11778.
[52] X. Chen, S. Sun, X. Wang, F. Li, D. Xia, J. Phys. Chem. C 116 (2012) 22737–22742.
[53] L. Osmieri, R. Escudero-Cid, A.H.A. Monteverde Videla, P. Ocón, S. Specchia, Appl. Catal. B: Environ. 201 (2017) 253–265.
[54] T. Kitahara, H. Nakajima, M. Inamoto, M. Morishita, J. Power Sources 234 (2013) 129–138.
[55] D. Spernjak, R. Mukundan, R.L. Borup, et al., ACS Appl. Energy Mater. 1 (2018) 6006–6017.
[56] B. Zahiri, R.M. Felix, A. Hill, et al., Appl. Surf. Sci. 458 (2018) 32–42.
[57] H.F. Lee, P.C. Wang, Y.W. Chen-Yang, J. Solid State Electrochem. 23 (2019) 971–984.
[58] H. Tang, S. Wang, M. Pan, R. Yuan, J. Power Sources 166 (2007) 41–46.
[59] H. Liu, W. Yang, J. Tan, Y. An, L. Cheng, Energy Conv. Manag. 176 (2018) 99–109.
[60] D. Qiu, L. Peng, P. Yi, X. Lai, W. Lehnert, Energy Conv. Manag. 174 (2018) 814–823.
[61] B. Timurkutluk, M.Z. Chowdhury, Fuel Cells 18 (2018) 441–448.

[62] J. Shen, Z. Tu, S.H. Chan, Appl. Therm. Eng. 149 (2019) 1408–1418.
[63] J. Song, H. Guo, F. Ye, C.F. Ma, Int. J. Energy Res. 43 (2019) 2940–2962.
[64] L.E. Asp, Plast. Rubber Compos. 42 (2013) 144–149.
[65] S.M. Kim, Y.S. Kang, C. Ahn, et al., J. Power Sources 317 (2016) 19–24.
[66] X. Liu, Y. Li, J. Xue, et al., Nat. Commun. 10 (2019) 842.
[67] D.-.H. Lee, W. Jo, S. Yuk, et al., ACS Appl. Mater. Interfaces 10 (2018) 4682–4688.
[68] Y. Zeng, H. Zhang, Z. Wang, et al., J. Mater. Chem. A 6 (2018) 6521–6533.
[69] I.M. Kong, J.W. Choi, S.I. Kim, E.S. Lee, M.S. Kim, Appl. Energy 145 (2015) 345–353.
[70] P. Trogadas, J.I.S. Cho, T.P. Neville, et al., Energy Environ. Sci. 11 (2018) 136–143.
[71] J. Dai, H.Thomas T. Hahn, Compos. Struct. 61 (2003) 247–253.
[72] E.E. Gdoutos, I.M. Daniel, Appl. Mech. Mater. 13-14 (2008) 91–98.
[73] J.T. South, R.H. Carter, J.F. Snyder, C.D. Hilton, D.J. O'Brien, E.D. Wetzel, Multi-functional power-generating and energy-storing structural composites for US Army applications, in: M. Chipara, D.L. Edwards, R.S. Benson, S. Phillips (Eds.), Materials For Space Applications, 2005, pp. 139–150.
[74] C.D. Hilton, D.M. Peairs, J.J. Lesko, S.W. Case, J. Fuel Cell Sci. Technol. 8 (2011) 051008.
[75] F. Wang, Q. Han, Z. Yi, et al., J. Electroanal. Chem. 807 (2017) 196–202.
[76] Q. Han, X. Li, F. Wang, et al., J. Electroanal. Chem. 833 (2019) 39–46.
[77] Q. Han, W. Zhang, Z. Han, et al., Ionics (Kiel) 25 (2019) 5333–5340.
[78] Q. Han, F. Wang, Z. Wang, et al., Ionics (Kiel) 24 (2017) 1049–1055.
[79] Q. Han, W. Zhang, Z. Han, et al., J. Mater. Sci. 54 (2019) 11972–11982.
[80] H. Li, S. Wang, M. Feng, J. Yang, B. Zhang, Chin. Chem. Lett. 30 (2019) 529–532.
[81] J. Liu, K. Song, P.A. van Aken, J. Maier, Y. Yu, Nano Lett. 14 (2014) 2597–2603.
[82] J. Hagberg, H.A. Maples, K.S.P. Alvim, et al., Compos. Sci. Technol. 162 (2018) 235–243.
[83] X. Tian, J. Jin, S. Yuan, et al., Adv. Energy Mater. 7 (2017) 1700127.
[84] K. Sun, T.S. Wei, B.Y. Ahn, et al., Adv. Mater. 25 (2013) 4539–4543.
[85] J.H. Pikul, H. Gang Zhang, J. Cho, P.V. Braun, W.P. King, Nat. Commun. 4 (2013) 1732.
[86] C. Sun, S. Liu, X. Shi, et al., Chem. Eng. J. 381 (2020) 122641.
[87] Y. Zhang, J. Ma, A.K. Singh, et al., J. Intell. Mater. Syst. Struct. 28 (2017) 1603–1613.
[88] T. Carlson, L. Asp, V. Ekermo, P.I. Sellergren, in: ICCM19, 2013.
[89] https://www.media.volvocars.com/global/en-gb/media/pressreleases/35026 (Accessed 5 September 2020).
[90] R. Wang, W. Cui, F. Chu, F. Wu, J. Energy Chem. 48 (2020) 145–159.
[91] X.B. Cheng, R. Zhang, C.Z. Zhao, Q. Zhang, Chem. Rev. 117 (2017) 10403–10473.
[92] D. Lin, Y. Liu, Z. Liang, et al., Nat. Nanotechnol. 11 (2016) 626.
[93] R. Zhang, X. Chen, X. Shen, et al., Joule 2 (2018) 764–777.
[94] X. Liu, X. Qian, W. Tang, et al., J. Energy Chem. 52 (2021) 385–392.
[95] P. Xue, C. Sun, H. Li, J. Liang, C. Lai, Adv. Sci. 6 (2019) 1900943.
[96] C. Yang, L. Zhang, B. Liu, et al., Proc. Natl. Acad. Sci. U. S. A. 115 (2018) 3770–3775.
[97] F. Li, J. He, J. Liu, et al., Angew. Chem., Int. Ed. 60 (2021) 6600–6608.
[98] H. Wang, J. He, J. Liu, et al., Adv. Funct. Mater. 31 (2021) 2002578.
[99] S. Qi, H. Wang, J. He, et al., Sci. Bull. 66 (2021) 685–693.
[100] N. Shirshova, H. Qian, M. Houlle, et al., Faraday Discuss 172 (2014) 81–103.
[101] Q. Li, L. Deng, J.K. Kim, et al., J. Electrochem. Soc. 164 (2017) A3220–A3228.
[102] Q. Li, Y.Q. Zhu, S.J. Eichhorn, J. Mater. Sci. 53 (2018) 14598–14607.
[103] A. Javaid, M.B. Zafrullah, F.uU.H. Khan, G.M. Bhatti, J. Compos Mater. 53 (2018) 1401–1409.
[104] H. Qian, A.R. Kucernak, E.S. Greenhalgh, A. Bismarck, M.S. Shaffer, ACS Appl. Mater. Interfaces 5 (2013) 6113–6122.
[105] A. Javaid, K.K.C. Ho, A. Bismarck, et al., J. Compos. Mater. 52 (2018) 3085–3097.
[106] Y. Wang, X. Qiao, C. Zhang, X. Zhou, J. Energy Storage 26 (2019) 100968.
[107] N. Shirshova, A. Bismarck, S. Carreyette, et al., J. Mater. Chem A 1 (2013) 15300–15309.
[108] X. Liu, R. Jervis, R.C. Maher, et al., Adv. Mater. Technol. 1 (2016) 1600167.
[109] W. Li, Y. Li, M. Su, et al., J. Mater. Chem. A 5 (2017) 16281–16288.
[110] Z. Niu, P. Luan, Q. Shao, et al., Energy Environ. Sci. 5 (2012) 8726–8733.
[111] X. Cao, B. Zheng, W. Shi, et al., Adv. Mater. 27 (2015) 4695–4701.
[112] J.X. Feng, S.H. Ye, A.L. Wang, et al., Adv. Funct. Mater. 24 (2014) 7093–7101.
[113] J.A. Lee, M.K. Shin, S.H. Kim, et al., ACS Nano 6 (2012) 327–334.
[114] W. Liu, M. Zhu, J. Liu, X. Li, J. Liu, Chin. Chem. Lett. 30 (2019) 750–756.
[115] R. Wang, Q.R. Wang, M.J. Yao, et al., Rare Met. 37 (2018) 536–542.
[116] L. Kou, T. Huang, B. Zheng, et al., Nat. Commun. 5 (2014) 3754.
[117] Y. Meng, Y. Zhao, C. Hu, et al., Adv. Mater. 25 (2013) 2326–2331.
[118] Z. Cai, L. Li, J. Ren, et al., J. Mater. Chem. A 1 (2013) 258–261.
[119] X. Chen, L. Qiu, J. Ren, et al., Adv. Mater. 25 (2013) 6436–6441.
[120] G. Qu, J. Cheng, X. Li, et al., Adv. Mater. 28 (2016) 3646–3652.
[121] M. Liao, H. Sun, J. Zhang, et al., Small 14 (2018) 1702052.
[122] L. Wang, Q. Wu, Z. Zhang, et al., J. Mater. Chem A 4 (2016) 3217–3222.
[123] H. Sun, X. Fu, S. Xie, et al., Adv. Mater. 28 (2016) 6429–6435.
[124] H. Sun, S. Xie, Y. Li, et al., Adv. Mater. 28 (2016) 8431–8438.
[125] Y. Hong, X.L. Cheng, G.J. Liu, et al., Chin. J. Polym. Sci. 37 (2019) 737–743.
[126] Y. Zhao, J. Cao, Y. Zhang, H. Peng, Adv. Funct. Mater. 30 (2019) 1902971.
[127] W.W. Ning, L.B. Chen, W. Wei, Y.J. Chen, X.Y. Zhang, Rare Met. 39 (2020) 1034–1044.
[128] Y. Wang, W. Zhou, Q. Kang, et al., ACS Appl. Mater. Interfaces 10 (2018) 27001–27008.
[129] S. Chen, B. Shi, W. He, et al., Adv. Funct. Mater. 29 (2019) 1906618.